MNRAS **446,** 1090–1097 (2015) doi:10.1093/mnras/stu2161

Measuring polarization in microlensing events

G. Ingrosso,[1,2]★ S. Calchi Novati,[3,4,5]† F. De Paolis,[1,2] Ph. Jetzer,[6] A. A. Nucita[1,2] and F. Strafella[1,2]

[1]*Dipartimento di Matematica e Fisica, 'Ennio De Giorgi', Università del Salento, CP 193, I-73100 Lecce, Italy*
[2]*INFN Sezione di Lecce, CP 193, I-73100 Lecce, Italy*
[3]*Dipartimento di Fisica 'E. R. Caianiello', Universitá degli Studi di Salerno, Via Giovanni Paolo II, 132, I-84084 Fisciano (SA) - Italy*
[4]*Istituto Internazionale per gli Alti Studi Scientifici (IIASS), via G. Pellegrino 19, I-84019 Vietri Sul Mare (SA), Italy*
[5]*NASA Exoplanet Science Institute, MS 100-22, California Institute of Technology, Pasadena, CA 91125, USA*
[6]*Physics Department, University of Zürich, Winterthurerstrasse 190, CH-8057 Zürich, Switzerland*

Accepted 2014 October 13. Received 2014 October 13; in original form 2014 July 1

ABSTRACT

We reconsider the polarization of the star light that may arise during microlensing events due to the high gradient of magnification across the atmosphere of the source star, by exploring the full range of microlensing and stellar physical parameters. Since it is already known that only cool evolved giant stars give rise to the highest polarization signals, we follow the model by Simmons et al. to compute the polarization as due to the photon scattering on dust grains in the stellar wind. Motivated by the possibility to perform a polarization measurement during an ongoing microlensing event, we consider the recently reported event catalogue by the Optical Gravitational Lensing Experiment (OGLE) collaboration covering the 2001–2009 campaigns (OGLE-III events), that makes available the largest and more comprehensive set of single-lens microlensing events towards the Galactic bulge. The study of these events, integrated by a Monte Carlo analysis, allows us to estimate the expected polarization profiles and to predict for which source stars and at which time is most convenient to perform a polarization measurement in an ongoing event. We find that about two dozens of OGLE-III events (about 1 per cent of the total) have maximum polarization degree in the range $0.1 < P_{\rm max} < 1$ per cent, corresponding to source stars with apparent magnitude $I \lesssim 14.5$, being very cool red giants. This signal is measurable by using the FOcal Reducer and low dispersion Spectrograph (FORS2) polarimeter at Very Large Telescope (VLT) telescope with about 1 h integration time.

Key words: polarization – Galaxy: bulge.

1 INTRODUCTION

It is well known that the light received from the stars is linearly polarized by the photon scattering occurring in the stellar atmospheres. The mechanism is particularly effective for the hot stars that have a free electron atmosphere, giving rise to a maximum polarization degree that can be as high as about 12 per cent at the stellar limb (Chandrasekhar 1960). By a minor extent, polarization may be also induced in main-sequence stars (of late type) by the scattering of star light off atoms and molecules (Fluri & Stenflo 1999) and in evolved, cool giant stars by photon scattering on dust grains contained in their extended envelopes powered by strong stellar winds (Simmons, Newsam & Willis 1995a).

The idea that the polarization could be enhanced by the microlensing effect at a level eventually above the instrumental threshold was first investigated in relation to supernovae by Schneider & Wagoner (1987). Then, Simmons et al. (1995a), Simmons, Willis & Newsam (1995b) and Bogdanov, Cherepashchuk & Sazhin (1996) presented a numerical calculation of the polarization induced by a single-lens (the Schwarzschild lens) microlensing a hot source star. The maximum polarization degree was found to be about 0.1 per cent. Hence, Agol (1996) calculated the time-dependent polarization of a hot star being microlensed by a binary system and found that polarization signals as high as $P \simeq 1$ per cent can be achieved when the source crosses in the lens plane a caustic (Schneider, Ehlers & Falco 1992) or passes near a cusp (Schneider & Weiss 1992; Zakharov 1995).

From an observational perspective, the more promising line of sight for detecting polarization signals associated with microlensing events is that towards the Galactic bulge where by now each year of order 1000 new events are reported, with the primary scientific goal being the search and characterization of exoplanets (Dominik 2010; Gaudi 2010). Along that line of sight, however, we expect a few or none hot giant source stars. Rather, it is expected that the highest polarization signals occur for microlensed cool, giant

★ E-mail: ingrosso@le.infn.it
† Sagan Visiting Fellow.

stars endowed with extended dust grain envelopes (Ingrosso et al. 2012). Indeed, these evolved stars constitute a significant fraction of the lensed sources in events towards the Galactic bulge, the LMC (Alcock et al. 1997; Moniez 2010) and the M31 galaxy (Calchi Novati 2010; Calchi Novati et al. 2014).

A useful formalism to evaluate the polarization profiles towards microlensed cool giant source stars has been developed by Simmons et al. (2002) for single-lens events and by Ignace, Bjorkman & Bryce (2006) for binary events. It turned out that the polarization degree ultimately depends on the dust optical depth τ and that for large enough values of $\tau \simeq 10^{-1}$ the polarization degree might become close to that expected for hot giant stars.

In a recent work (Ingrosso et al. 2012), a specific set of highly magnified, single-lens events (Choi et al. 2011) was considered along with a subset of exoplanetary events observed towards the Galactic bulge (Dominik 2010; Gaudi 2010). For these events, the polarization profiles as a function of time were calculated, taking into account the nature of the source stars (a main sequence of late type or a cool giant star) and it was shown that the currently available technology may potentially allow the detection of such signals.

Besides the interest related to stellar astrophysics, the observation of the polarization variability may in principle provide independent constraints on the lensing parameters. Indeed, it was shown (Ingrosso et al. 2014) that polarization measurements may allow us to distinguish between binary and exoplanetary[1] lens solutions that are degenerate solutions when looking merely to the observed light curves.

In this paper, also in view of the fact that highly magnified events considered in our previous works are not so frequent, we extend the analysis of the expected polarization signal for single-lens events towards the Galactic bulge, covering the full range of microlensing parameters.

Concerning the polarization mechanism in operation, it is clear from our analysis (Ingrosso et al. 2012) that, due to paucity of hot stars in the Galactic bulge, the source stars with the highest chance to give rise to a non negligible polarization signal are cool, evolved giants, for which the photon scattering on dust grains is the leading polarization mechanism.

Therefore, following the model by Simmons et al. (2002), briefly summarized in Section 2, we assume that dust grains may form in the stellar atmospheres, beyond the distance $R_{\rm h}$ greater than the source radius $R_{\rm S}$, at which the gas temperature becomes lower than the dust sublimation temperature. The model is characterized by the presence of an internal cavity (between $R_{\rm S}$ and $R_{\rm h}$) devoid of dust, giving rise during a microlensing event to two different polarization profiles, as a function of the time t, for *bypass* and *transit* events (Simmons et al. 1995a,b). Indeed, when the trajectory (projected in the lens plane) of the cavity remains outside the lens (*bypass* events), one obtains a bell-like polarization profile with the peak occurring at the instant of maximum magnification t_0. When a part of the cavity is aligned with the lens and the observer (*transit* events), the polarization curve presents two maxima and one minimum (in correspondence to t_0). The polarization signal gets the two maximum values when the cavity enters and exits the lens.

Note that a major advantage of considering the polarization (namely the microlensing of the envelope instead of the stellar disc) is that the probability for observing finite source effects in microlensing events increases (Yoshida 2006). Indeed, in the case of *bypass* events, for which the trajectory of the source disc does not intersects the lens, the finite source effects, negligible on the event light curves – that are not sensitive to the limb-darkening phenomena (Gaudi & Gould 1999; Heyrovský & Sasselov 2000; Abe et al. 2003) – produce a polarization signal that constitute, therefore, a unique probe of the stellar atmosphere. In *transit* events for which the source disc transverses the lens, the finite source effects manifest themselves in the polarization variability when the internal cavity transits the lens, while in the light curves their effects may appear or not depending on the sensitivity of the light curve to the limb-darkening phenomenon (Gaudi & Gould 1999; Heyrovský & Sasselov 2000; Abe et al. 2003).

Our present analysis of the polarization runs along two parallel paths, the first being a study of the signal present in microlensing events generated by using a Monte Carlo code. This preliminary study allows us to clarify the dependence of the polarization signal on the microlensing parameters and the physical parameters of the source stars.

Then we consider the set of OGLE-III events relative to the 2001–2009 observational campaign towards the Galactic bulge recently reported in Wyrzykowski et al. (2014) with an evaluation of the expected polarization signal. This analysis is however complemented by a Monte Carlo study, since the observational data alone do not allow us to completely characterize the polarization signal.

The overall analysis eventually leads us to determine the physics that can be extracted by the study of the polarization as well as the optimal observational strategy for forthcoming microlensing events. Indeed, our final aim is to design an observational strategy which allows us to maximize the chance of positive polarization measurements with an observational programme based on the current microlensing surveys. To this aim we consider the OGLE-III event catalogue recently presented by Wyrzykowski et al. (2014). All these available data allow us to compute the maximum polarization degree in each of the observed events and the best time to perform a polarization measurement in an ongoing event, once an alert system has predicted the instant of the occurrence of the magnification peak. This, in turn, also makes possible to estimate that for a few events per year (about 1 per cent of the OGLE-III events) the FORS2 polarimeter on VLT telescope, in 1 h of integration time, may allow us to obtain a positive polarization measurement with $P_{\rm max} > 0.1$ per cent (see Section 5).

2 POLARIZATION MODEL

Following the approach in Chandrasekhar (1960), we consider the linear polarization of the star light scattered in a stellar atmosphere. We define the intensities $I_l(\mu)$ and $I_r(\mu)$ emitted in the direction making an angle $\chi = \arccos(\mu)$ with the normal to the star surface and polarized as follows: $I_l(\mu)$ is the intensity in the plane containing the line of sight and the normal, $I_r(\mu)$ is the intensity in the direction perpendicular to this plane (light propagates in the direction $\boldsymbol{r} \times \boldsymbol{l}$).

To calculate the polarization of a star with centre at projected position $(p_{\rm S}, \varphi_{\rm S})$ in the lens plane, we integrate the unnormalized Stokes parameters and the flux over the star disc (Simmons et al. 1995a,b; Agol 1996)

$$F = F_0 \int_0^{2\pi} \int_0^{\infty} A(p,\varphi)\, I_+(\mu)\, p \mathrm{d}p\, \mathrm{d}\varphi\,, \tag{1}$$

$$F_Q = F_0 \int_0^{2\pi} \int_0^{\infty} A(p,\varphi)\, I_-(\mu)\, \cos 2\varphi\, p \mathrm{d}p\, \mathrm{d}\varphi\,, \tag{2}$$

[1] Exoplanetary events are binary lens systems characterized by values of the planet-to-star mass ratio $q \ll 1$ and smaller star-to-planet distance d as compared to the separation of the stars in a binary system.

$$F_U = F_0 \int_0^{2\pi} \int_0^{\infty} A(p,\varphi)\, I_-(\mu)\, \sin 2\varphi\; p\mathrm{d}p\, \mathrm{d}\varphi\,, \tag{3}$$

where F_0 is the unamplified star flux, $A(p, \varphi)$ the point source magnification and

$$I_+(\mu) = I_r(\mu) + I_l(\mu)\,, \tag{4}$$

$$I_-(\mu) = I_r(\mu) - I_l(\mu)\,. \tag{5}$$

As usual, the polarization degree is given by $P = (F_Q^2 + F_U^2)^{1/2}/F$.

We use a coordinate system with the lens at the origin O and with the source trajectory along the x-axis. The location of a point (p, φ) on the star surface is determined by the distance p from the star centre and by the angle φ formed with the Ox-axis. Since we are considering single-lens events, for each surface element on the stellar disc the magnification is given by (Einstein 1936; Paczyński 1986)

$$A = \frac{u^2+2}{u\sqrt{u^2+4}}\,, \tag{6}$$

where u is the distance, in units of the Einstein radius R_E, between the considered surface element and the lens position

$$u = \sqrt{p_\mathrm{S}^2 + p^2 - 2pp_\mathrm{S}\cos(\varphi - \varphi_\mathrm{S})}\,. \tag{7}$$

Here, $R_\mathrm{E} = [(4Gm_\mathrm{L}/c^2)(D_\mathrm{L}/D_\mathrm{S})(1 - D_\mathrm{L}/D_\mathrm{S})]^{1/2}$, being m_L the lens mass and D_S (D_L) the source (lens) distance from the observer.

Clearly, by taking into account the finite source effect, the overall source magnification is obtained by integration on the distance $\bar{R}_\mathrm{S} = (R_\mathrm{S}/R_\mathrm{E})(D_\mathrm{L}/D_\mathrm{S})$ (the physical radius R_S, in units of R_E, projected in the lens plane)

$$\langle A\rangle = \frac{\int_0^{2\pi}\int_0^{\bar{R}_\mathrm{S}} A(p,\varphi)\; p\mathrm{d}p\, \mathrm{d}\varphi}{\int_0^{2\pi}\int_0^{\bar{R}_\mathrm{S}} p\mathrm{d}p\, \mathrm{d}\varphi}\,. \tag{8}$$

The light-curve and polarization profiles as a function of the time t are obtained by specifying in the above equations the time-dependent position of the source star centre

$$p_\mathrm{S} = \sqrt{u_0^2 + [(t-t_0)/t_\mathrm{E}]^2}\;, \quad \varphi_\mathrm{S} = \arctan\frac{u_0}{(t-t_0)/t_\mathrm{E}}\,, \tag{9}$$

where u_0 is the lens impact parameter, t_0 the maximum magnification time and t_E the Einstein time.

The explicit form of the intensities $I_+(\mu)$ and $I_-(\mu)$ is given in Simmons et al. (2002) and Ignace et al. (2006). It turns out that the polarization P linearly depends on the dust optical depth

$$\tau = n_\mathrm{h}\sigma R_\mathrm{h}/(\beta - 1)\,, \tag{10}$$

in the limit of $\tau \ll 1$. Here, σ is the scattering cross-section (evaluated in the dipole approximation) of photons off dust grains, R_h is the distance at which dust grains may form in the stellar wind and the scatterers are taken to have a number density decreasing with the distance (from the n_h value) with a power law of exponent β.

We estimate the distance R_h according to simple energy balance criteria by considering the balance between the energy absorbed and emitted by a typical dust grain as a function of the distance r from the star centre

$$\int_0^{\infty} F_\lambda^\mathrm{S}(r)\pi a^2 Q_\lambda \mathrm{d}\lambda = \int_0^{\infty} 4\pi a^2 \pi B_\lambda[T(r)] Q_\lambda \mathrm{d}\lambda\,, \tag{11}$$

where $F_\lambda^\mathrm{S}(r)$ is the stellar flux at distance r

$$F_\lambda^\mathrm{S}(r) = \left(\frac{R_\mathrm{S}}{r}\right)^2 \pi B_\lambda(T_\mathrm{eff})\,. \tag{12}$$

Here, T_eff is the effective temperature of the source star, B_λ the blackbody emissivity at the wavelength λ, Q_λ the grain absorption efficiency, $T(r)$ the dust temperature at distance r and a the dust grain size. This calculation assumes that the heating by non-radiative processes and by the diffuse radiation field is negligible so that we limited ourselves to compute Q_λ for a typical particle size distribution (Mathis, Rumpl & Nordsiek 1977) with optical constants derived by Draine & Lee (1984). Specifically, the numerical values for R_h are obtained by using equation (11) with $T_\mathrm{h} \equiv T(R_\mathrm{h}) \simeq 1400$ K.

Concerning the dust optical depth, it was found that the dependence of τ from stellar and wind parameters can be approximated by (Ignace, Bjorkman & Bunker 2008)

$$\tau = 2\times10^{-3}\eta\mathcal{K}\left(\frac{\dot{M}}{10^{-9}\,\mathrm{M_\odot\,yr^{-1}}}\right) \times\left(\frac{30\,\mathrm{km\,s^{-1}}}{v_\infty}\right)\left(\frac{24\,\mathrm{R_\odot}}{R_\mathrm{h}}\right), \tag{13}$$

where $\eta \simeq 0.01$ is the dust-to-gas mass density ratio, $\mathcal{K} \simeq 200\,\mathrm{cm^2\,g^{-1}}$ is the dust opacity at $\lambda > 5500$ Å, $\dot{M}$ is the mass-loss rate and v_∞ is the asymptotic wind velocity. Observational data indicate that v_∞ is related to the escape velocity $v_\mathrm{esc} = \sqrt{2GM_\mathrm{S}/R_\mathrm{S}}$, depending on the source spectral and luminosity class. In particular, $v_\infty \simeq 0.2 v_\mathrm{esc}$ in the case of asymptotic giant branch (AGB) stars (Marshall et al. 2004) that are the sources giving the highest polarization signals.

We can relate $\dot{M}$ in equation (13) to the luminosity L, gravity g and radius R of the magnified source star. Indeed, it is well known that from main sequence to AGB phase stars, the mass-loss rate $\dot{M}$ increases by several orders of magnitude. Here, we adopt the simple empirical mass-loss rate relation (Reimers 1975)[2]

$$\dot{M} = \eta_R\, 4\times10^{-13}\,\frac{(\mathrm{L/L_\odot})}{(g/g_\odot)\,(R/\mathrm{R_\odot})}\,(\mathrm{M_\odot\,yr^{-1}})\,. \tag{14}$$

where $\mathrm{L_\odot}$, $g_\odot$ and $\mathrm{R_\odot}$ are luminosity, gravity and radius for the Sun, respectively, and η_R is a free parameter that is estimated by a best-fitting procedure to the observational data, being $\eta_R \simeq 0.3$ for late-type main-sequence stars and $\eta_R \simeq 3$ for red giant stars.

By assuming the relation in equation (14), values of $\dot{M}$ in the range $(10^{-12}$–$10^{-8})\,\mathrm{M_\odot\,yr^{-1}}$ are obtained for typical stars evolving from main-sequence to red giant star phases.

Before closing this section we remark that, as it is well known, in analysing microlensing observations, the parameters t_0, u_0, t_E (and, possibly, $\bar{R}_\mathrm{S}$ for events with large finite source effects) are determined by fitting each light curve with the Paczyński (1986) law, while the distances D_S, D_L and R_E remain undetermined. Then, also given the R_S and R_h physical radii, the adimensional distances $\bar{R}_\mathrm{h} = (R_\mathrm{h}/R_\mathrm{E})(D_\mathrm{L}/D_\mathrm{S})$ and $\bar{R}_\mathrm{S}$ (for events with negligible finite source effects) remain unknown, making not possible to compute the polarization signal raised in the microlensing event. The way out we adopt in the analysis of the observed OGLE-III events (Section 4.2) is to use a Monte Carlo code to determine the more likely values of D_S, D_L and R_E corresponding to the event t_E value.

[2] Here, we note that several different mass-loss rate relations are present in the literature obtained by fitting observational data – see e.g. Catelan (2000) – and by numerical models (Ferguson et al. 2005).

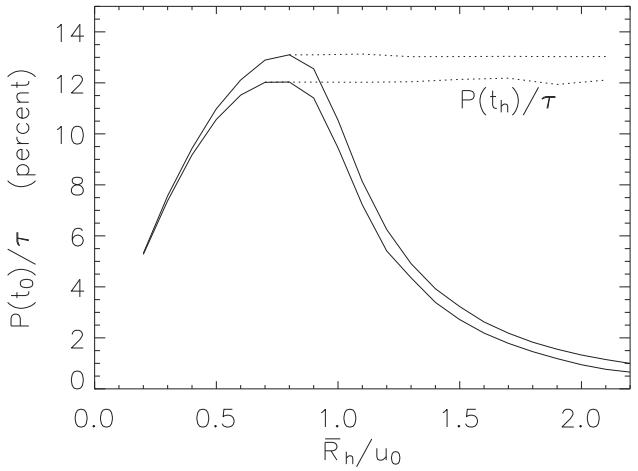

Figure 1. The ratio $P(t_0)/\tau$ in per cent at the time t_0 of maximum magnification is given (solid lines) as a function $\bar{R}_h/u_0$, assuming $\bar{R}_h/\bar{R}_S = 2,\ 5$ (from the bottom). For bypass events ($\bar{R}_h < 0.75u_0$), $P(t_0)/\tau$ is the maximum of the polarization variability as a function of the time t. In the case of transit events ($\bar{R}_h > 0.75u_0$), $P(t_0)/\tau$ is a local minimum of the polarization curve and the maximum value $P(t_h)/\tau \simeq 12.5$ occurs twice at the t_h instants given by equation (15).

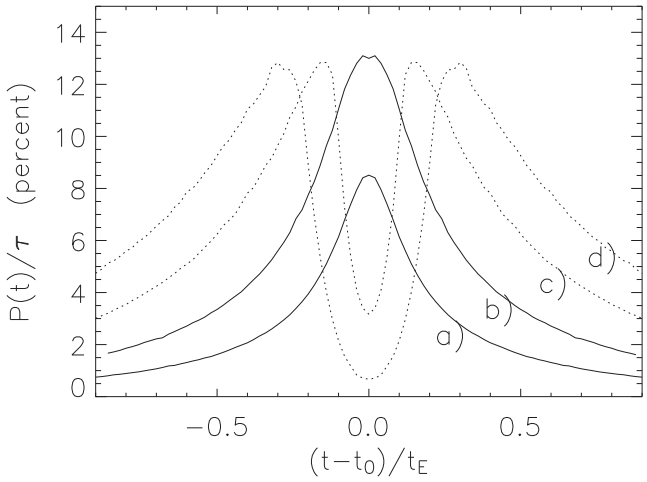

Figure 2. Assuming constant parameter values $u_0 = 0.09$, $t_E = 60$ d and $\bar{R}_h/\bar{R}_S = 5$, the $P(t)/\tau$ polarization curves are shown as a function of $(t - t_0)/t_E$, for increasing values of $\bar{R}_h/u_0 = 0.35,\ 0.75,\ 1.5,\ 2.5$, corresponding to curves labelled (a), (b), (c) and (d), respectively. Full lines – (a) and (b) – are bypass events, dotted lines – (c) and (d) – are transit events.

3 POLARIZATION RESULTS

In this section, we describe the dependence of the intensity and shape of the polarization signal from the microlensing parameters u_0 and t_E, and from the parameter ratios $\bar{R}_h/u_0$ and $\bar{R}_h/\bar{R}_S$.

At first we focus on the polarization signal $P(t_0)/\tau$ at the instant t_0 of maximum magnification, which is independent from the value of t_E. Fig. 1 shows[3] the ratio $P(t_0)/\tau$ in per cent as a function of $\bar{R}_h/u_0$. The curves are given for $\beta = 2$ and for two different values of $\bar{R}_h/\bar{R}_S = 2$ and 5. We have verified that in the limit $u_0 \ll 1$, the $P(t_0)/\tau$ profiles weakly depend on $\bar{R}_h/\bar{R}_S$ and any curve is inside the region bounded by the two curves plotted in Fig. 1. Therefore, the polarization level at the time t_0 depends only on the ratio $\bar{R}_h/u_0$, assuming the maximum value of about $P(t_0)/\tau \simeq 12.5$ per cent when $\bar{R}_h/u_0 \simeq 0.75$.

The effect of varying the model parameter β in equation (10) is shown in fig. 3 in Ingrosso et al. (2014), where one can see that increasing $\beta = 2, 3, 4$, the $P(t_0)/\tau$ values increase from 12.5 up to about 25 per cent. However, since $P(t_0)/\tau$ rapidly decreases outside the interval $0.1 < \bar{R}_h/u_0 < 2.2$, it is clear that the presence of a large enough polarization signal at t_0 requires that microlensing and stellar parameters u_0 and $\bar{R}_h$ be fine-tuned.

The ratio $\bar{R}_h/u_0$, not only determines the value of the polarization signal at t_0, but also the shape of the polarization profile $P(t)/\tau$ as a function of time, and in particular the possible existence of two polarization peaks at symmetrical positions with respect to t_0.

Indeed, when $\bar{R}_h/u_0 \lesssim 0.75$, i.e. for *bypass* events – for which the trajectory of the internal star cavity (devoid of dust grains) remains outside the lens – one obtains a bell-like polarization profile with the peak occurring at t_0.

For $\bar{R}_h/u_0 \gtrsim 0.75$, i.e. for *transit* events – where a part of the internal cavity is aligned with the lens and the observer – the polarization curve present two maxima and one minimum (in correspondence to t_0). The polarization signal gets the two maximum values when the internal cavity enters and exits the lens.

The different behaviour of the polarization profiles for *bypass* and *transit* events is clarified in Fig. 2 where, by taking constant values for the parameters u_0 and t_E, we show the $P(t)/\tau$ profiles as a function of the 'adimensional time' $(t - t_0)/t_E$, for increasing values of $\bar{R}_h/u_0$. As one can see in Fig. 2, the same maximum value of $P(t)/\tau \simeq 12.5$ per cent is achieved for the simulated event labelled by (b) (the limiting *bypass/transit* event with $\bar{R}_h/u_0 = 0.75$) and for events (c) and (d), that are two *transit* events with $\bar{R}_h/u_0 = 1.38$ and 2.06, respectively. The effect of varying in Fig. 2 the parameter t_E is to change the time-scale of the polarization variability, while the event nature (*transit* or *bypass*) remains unchanged.

This behaviour of the polarization profiles is indeed expected since for *transit* events the central value $P(t_0)/\tau$ corresponds to the minimum of the polarization curve – with intensity depending on $\bar{R}_h/u_0$ as shown in Fig. 1 – and, for increasing t, there always exists along the star trajectory two positions of the source star centre at which $\bar{R}_h/u_h \simeq 0.75$, being $u_h = \sqrt{u_0^2 + [(t_h - t_0)/t_E]^2}$. This clearly implies that the two polarization peaks occur at times

$$t_h = t_0 \pm t_E \sqrt{\left(\frac{\bar{R}_h}{0.75}\right)^2 - u_0^2}\,. \qquad (15)$$

It goes without saying that the apparent source star luminosity at t_h decreases with respect to the value at the maximum magnification time t_0, therefore making more hard performing a measurement of the polarization signal in events with relatively large values of $\bar{R}_h/u_0$.

4 OBSERVATIONAL OUTLOOK

This section aims to present a discussion of the observational perspectives to effectively perform a polarization measurement during an ongoing microlensing event.

Very recently, the OGLE collaboration presented the largest and more comprehensive catalogue of microlensing events ever constructed (Wyrzykowski et al. 2014). The sample of single-lens events comprises 3718 events towards the Galactic bulge for years 2001–2009 (OGLE-III campaigns), with 1410 events not detected

[3] We point out that in our previous analysis (Ingrosso et al. 2012) there was a mistake in using equation 13 in Simmons et al. (2002), that gives rise to a different $P(t_0)/\tau$ profile (shown in Fig. 1) with respect to that published in fig. 3 of Ingrosso et al. (2012).

before in real time by the Early Warning System of the OGLE experiment. The observed light curves have been re-analysed and new values of the microlensing parameters have been obtained. The microlensing event detection efficiency was also determined as a function of the Einstein time.

We first make a study (in Section 4.1) of the maximum polarization signal occurring in microlensing events generated by means of a Monte Carlo code. Then, we estimate (in Section 4.2) the polarization degree that would occur in the real OGLE-III events.

We remark that the Monte Carlo and OGLE-III analyses complement each other. In fact, starting from the full sample of Monte Carlo generated events, we make use of the OGLE-III event detection efficiency, so to draw our final sample of 'potentially observable' events. In turn, the Monte Carlo study allows us to determine in the OGLE-III analysis the unknown distance scales D_S, D_L and R_E, making possible to compute the polarization signal raised in the event.

4.1 Monte Carlo analysis

We generated a sample of microlensing events with source stars in the Galactic bulge and lenses either in the bulge or in the disc of the Galaxy. For the sake of simplicity, we assume sources at distance $D_S = 8$ kpc and the line of sight to the Galactic centre ($l = 0, b = 0$). The mass and the distance of the lenses and the velocity of both sources and lenses are selected, using a model for the distribution of the stars in the Galaxy, by means of the Monte Carlo technique (Ingrosso et al. 2006, 2007, 2009).

As a first step, we have verified that the obtained distribution of the Einstein time t_E is in agreement with the observational results, as given by fig. 7 in Wyrzykowski et al. (2014). Then, we use the OGLE-III event detection efficiency as a function of t_E (given in fig. 8 of the above cited paper) to select the 'potentially observable' events, starting from the full sample of generated events.

In the Monte Carlo analysis, we draw the source stars according to a synthetic luminosity function generated using the IAC-Star CMD code.[4] Here, we assume that the Galactic bulge stars were generated by a single starburst that occurred about 13 Gyr ago in a solar metallicity gas cloud and adopting a Kroupa et al. (1993) initial mass function. Then, for each star of our adopted catalogue we compute the cavity radius R_h by using equations (11) and (12) with the appropriate values of R_S and T_{eff}.[5]

We explore the full range of stellar luminosities and temperatures allowing the colour index $(V - I)_{int}$ to vary uniformly in the range $-5 < I_{int} < 0.5$, also including source stars that are not present in the OGLE-III catalogue of observed sources. Here and in the following we indicate with the subscript '$_{int}$' dereddened quantities of the unlensed source star.[6]

Given the physical parameters of the source stars, by using equations (13) and (14) we estimate the dust optical depth τ and in turn the maximum polarization degree given by $P_{max} \equiv P(t_{max}) \simeq 12.5\,\tau$ per cent, being $t_{max} = t_0$ for *bypass* events and $t_{max} = t_h$ for *transit* events (see Section 3.).

[4] http://iac-star.iac.es/cmd/www/form.htm

[5] Based on the model we use for R_h and T_h, we find the scatter plot R_h/R_S versus T_{eff} to follow the analytical relation $R_h/R_S = 0.45(T_{eff}/T_h)^{2.5}$ found by Lamers & Cassinelli (1999).

[6] We find a linear relation between the intrinsic colour index $(V - I)_{int}$ and the effective star temperature T_{eff}, which is consistent with the widely accepted analytical approximations in the literature (Sekiguchi & Fukugita 2000).

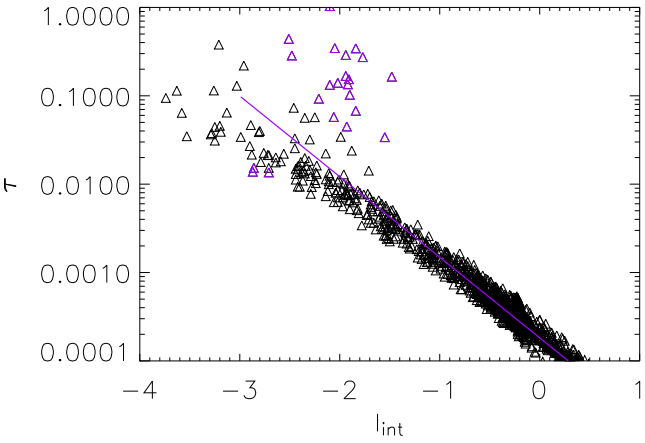

Figure 3. Scatter plot of the dust optical depth τ versus the source star intrinsic magnitude I_{int}.

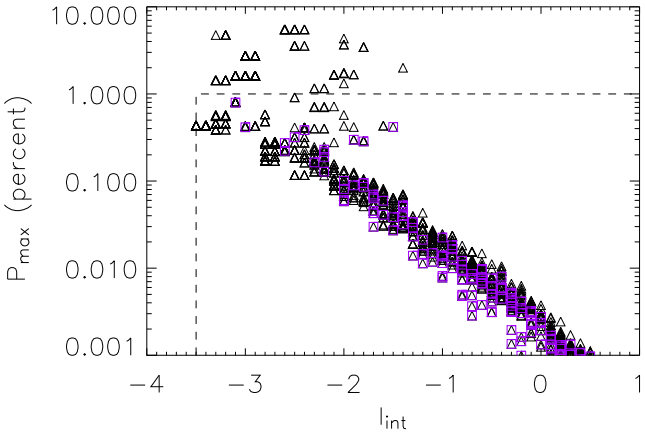

Figure 4. Scatter plot of P_{max} in per cent versus the unmagnified star magnitude I_{int} for simulated transit (triangles) and bypass (purple squares) events. The dashed lines delimit the region containing the results for the OGLE-III events (see Section 4.2).

The corresponding values of τ are shown in Fig. 3 where we give a scatter plot of τ versus I_{int}. In the same figure, for comparison purposes, we show a linear fit to the simulated data and, as coloured triangles, the points with τ values above two standard deviations with respect to the linear fit.

In Figs 4, 5 and 6, we give P_{max} as a function of I_{int}, T_{eff} and $(V - I)_{int}$ of the source stars, respectively. As one can see, we have $P_{max} < 1$ per cent for red giants with $(V - I)_{int} < 3$, which corresponds to $I_{int} > -3.5$ and $T_{eff} > 3500$ K (events inside the regions delimited by dashed lines). There are, however, a few events with $1 < P_{max} < 10$ per cent, characterized by $(V - I)_{int} > 3$ and $T_{eff} < 3500$ K, corresponding to source stars in the AGB phase. These stars, that are rather rare in the Galactic bulge, have not been as yet sources of microlensing events observed in the OGLE-III campaign.

In this respect, the expected significant increase in event rate by the forthcoming new generation bulge microlensing surveys [both ground-based, as KMTNet (Henderson et al. 2014), and from space, *EUCLID* (Penny et al. 2013) and *WFIRST* (Yee et al. 2014)] open the possibility to develop an alert system able to trigger polarization measurements in ongoing microlensing events with very bright sources.

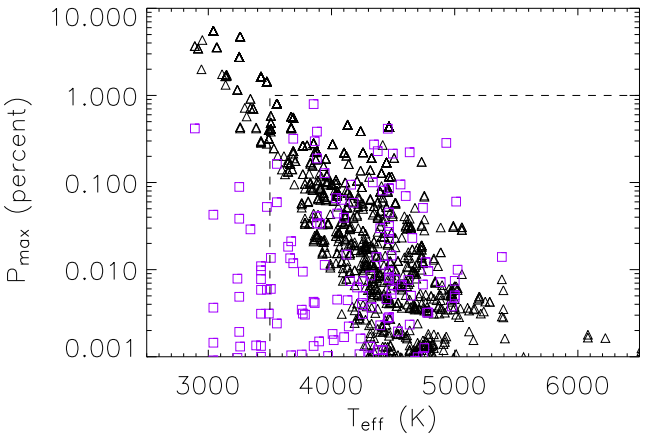

Figure 5. Scatter plot of P_{max} in per cent versus the source temperature T_{eff} for transit (triangles) and bypass (purple squares) events. The dashed lines delimit the region containing the results for the OGLE-III events (see Section 4.2).

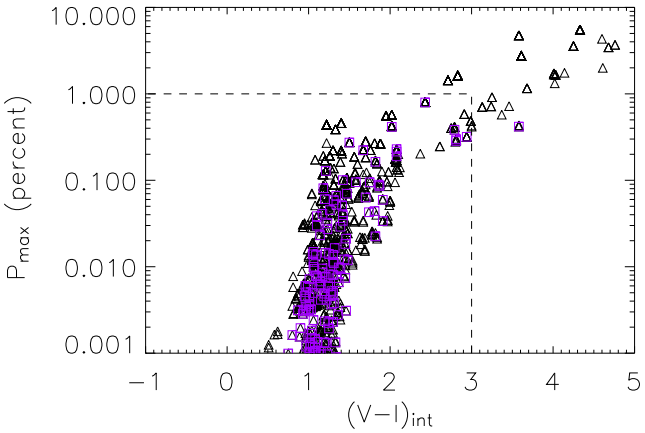

Figure 6. Scatter plot of P_{max} in per cent versus the colour index $(V-I)_{int}$ for simulated transit (triangles) and bypass (purple squares) events. The dashed lines delimit the region containing the results for the OGLE-III events (see Section 4.2).

4.2 OGLE-III events

We now consider the sample of single-lens OGLE-III events recently re-analysed by Wyrzykowski et al. (2014). Our aim is to compute the expected polarization signal in 2614 events (out of the 3718 total number) for which line of sight, microlensing parameters and baseline magnitudes in V and I bands of the source stars are given.

In the present analysis, we assume that the baseline magnitude and colour are reliable estimate of the source magnitude and colour, namely we are assuming blending is negligible. Despite this assumption is in general questionable, it is however reasonable at least for the brightest stars in the sample, that our analysis favours as the best candidates to produce appreciable polarization signals.

We derive the physical parameters of each microlensed source by assuming that the interstellar extinction A_I and the reddening $E(V-I)$ of each source star are those measured by Nataf et al. (2013) for the OGLE field of view towards the Galactic bulge nearest to the event line of sight. In this respect, we point out that attributing the average values of A_I and $E(V-I)$ in each field of view to the single sources may alter the true values of the stellar physical parameters, thereby producing a difference

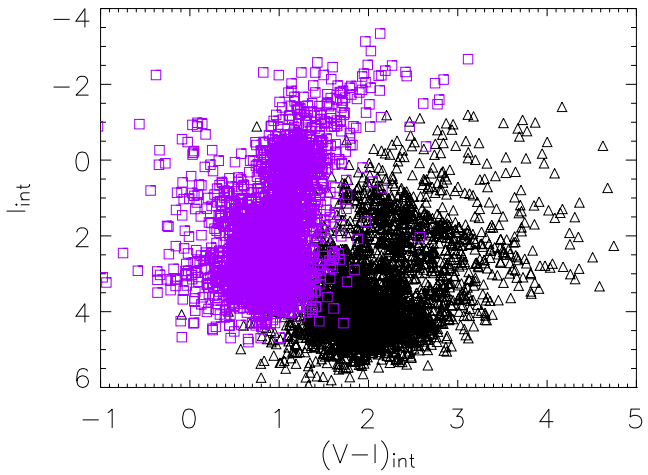

Figure 7. Scatter plot of I_{int} versus $(V-I)_{int}$ (purple squares) for the stars in the OGLE-III catalogue (Wyrzykowski et al. 2014) corrected for absorption and reddening. For comparison, we give also the scatter plot of the observed quantities I and $(V-I)$ (triangles).

in the estimated values of τ and ultimately of P_{max}. Indeed, this is exactly what happened in the case of the event OGLE-2011-BLG-1101/MOA-2011-BLG-325 (Ingrosso et al. 2012) for which $T_{eff} \simeq 5100$ K if it is estimated by using the catalogue in Nataf et al. (2013) while $T_{eff} \simeq 3800$ in Choi et al. (2011).

In Fig. 7, we give the scatter plot of the intrinsic magnitude $I_{int} = I - A_I$ versus the colour index $(V-I)_{int} = (V-I) + E(V-I)$. We observe that the distribution of the magnitude for the microlensed source stars is different from that of the bulge stars as an effect of the event selection criteria (Wyrzykowski et al. 2014).

The effective temperature T_{eff} of each source star is then evaluated since is known the relation between intrinsic colour index $(V-I)_{int}$ and T_{eff}. In turn, the stellar radius is calculated through the relation $L_{Bol} = 4\pi\sigma R_S^2 T_{eff}^4$, and finally the microlensed star mass is selected by searching in the IAC catalogue a star with the assigned values of I_{int}, T_{eff} and R_S. This allows us to estimate the mass-loss rate through equation (14) and finally τ as given by equation (13).

The OGLE-III event parameters by themselves do not allow us a complete characterization of the expected polarization signal, for which we need, in particular, a full knowledge of the microlensing event parameters. For this purpose, we here make use once again of the Monte Carlo model constrained by the observational data. Assuming a model for the distribution of sources and lens in the Galaxy, we generate, a synthetic microlensing event catalogue, by selecting the source (lens) distance D_S (D_L), the lens mass m_L and the relative (projected in the lens plane) velocity $v_\perp$ between the source and the lens (Ingrosso et al. 2006, 2007, 2009). Then, for each OGLE-III event, we select within the catalogue, the event having the ratio between R_E and $v_\perp$ (being $t_E = R_E/v_\perp$) nearest to the observed one. In this way we are able to evaluate the adimensional $\bar{R}_S$ and $\bar{R}_h$ radii.

For each of the considered OGLE-III events, we thereby compute the maximum polarization degree $P_{max} \equiv P(t_{max})$: $t_{max} = t_0$ for *bypass* events, $t_{max} = t_h$ for *transit* events. All events have $P_{max} < 1$ per cent and only a few dozens have $0.1 < P_{max} < 1$ per cent. The obtained scatter plots of P_{max} versus I_{int}, T_{eff} and $(V-I)_{int}$ (not given) are similar to those obtained for Monte Carlo events shown in the Figs 4, 5 and 6, with data points inside the region $P_{max} < 1$ per cent, $I_{int} > -3.5$, $T_{eff} > 3500$ K and $(V-I)_{int} < 3$, respectively. The lack of events in the OGLE-III

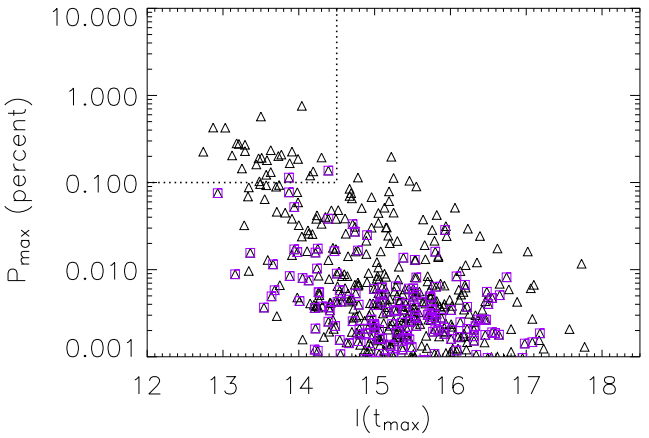

Figure 8. Maximum polarization expected in OGLE-III events. $P_{\max}$ in per cent is given versus the apparent magnitude $I(t_{\max})$. either for transit (triangles) and bypass (purple squares) events. The region enclosed in dashed lines shows the more favourable events (about 1 per cent of the OGLE-III events) for polarization measurements, assuming 1 h integration time with FORS2 at ESO-VLT telescope.

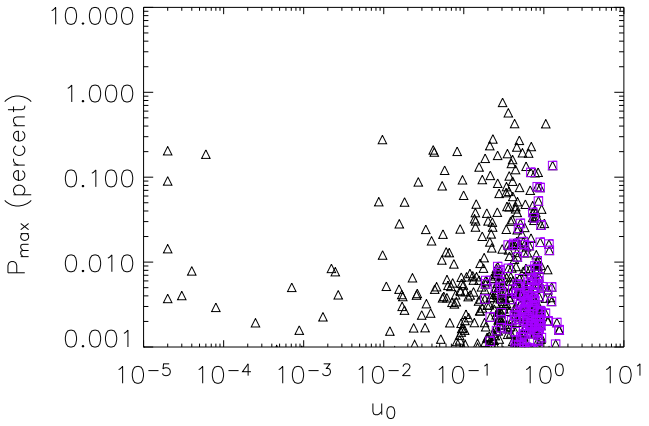

Figure 9. Scatter plot of $P_{\max}$ versus the impact parameter u_0 either for transit (triangles) and bypass (purple squares) OGLE-III.

catalogue with $P_{\max} > 1$ per cent is clearly due to the paucity of bulge AGB stars implying that none of them has been microlensed during the 2001–2009 campaigns.

In Fig. 8, the maximum polarization degree $P_{\max}$ expected for the OGLE-III events is given as a function of the stellar apparent magnitude $I_{\max}$ at the time instant of maximum polarization. The region enclosed in dotted lines shows the more favourable events (about 1 per cent of the OGLE-III events) for polarization measurements, assuming 1 h integration time with FORS2 at ESO-VLT telescope (Ingrosso et al. 2012).

The event distribution with the impact parameter is shown in Fig. 9, where one can see that *transit* events have higher polarization signals with respect to *bypass* ones. This figure also shows that the same polarization level is achieved in events with low and high magnification. Finally, in Fig. 10, for *transit* events, we show the increase of apparent magnitude $\Delta I = I(t_{\rm h}) - I(t_0)$ between the time instant $t_{\rm h}$ of maximum polarization and t_0 of maximum magnification: ΔI increases with increasing $\bar{R}_{\rm h}/u_0$ and this makes more hard to measure the polarization in events with large values of $\bar{R}_{\rm h}/u_0$.

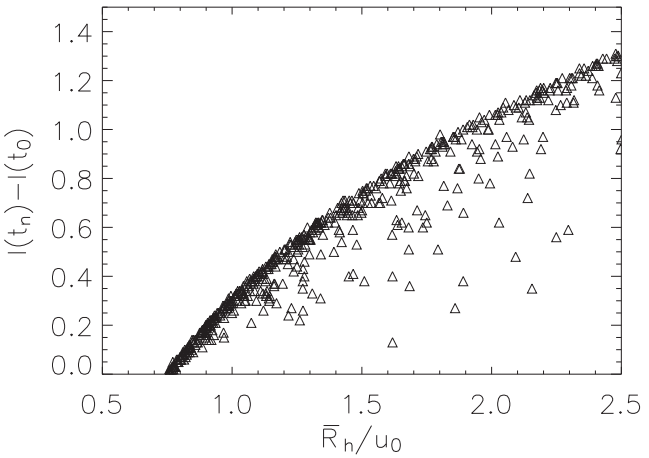

Figure 10. For transit events, the increase of source magnitude $I_{\rm int}(t_{\rm h}) - I_{\rm int}(t_0)$ at the instant $t_{\rm h}$ of maximum polarization with respect the instant t_0 of maximum magnification is shown as a function of $\bar{R}_{\rm h}/u_0$.

5 SUMMARY AND CONCLUSIONS

The study of the OGLE-III microlensing events towards the Galactic bulge recently reported by Wyrzykowski et al. (2014), integrated by a Monte Carlo analysis, allows us to compute the expected polarization signal for a large number of events (2616 out of 3718 events) for which all the physical parameters of the source stars can be determined.

We focus on cool giant source stars, as they provide a higher level of polarization, and we follow the model by Simmons et al. (2002) for which the polarization degree P is proportional to the dust optical depth τ. This quantity, computed by using the relations in equations (13) and (14), is found in the range $10^{-4} < \tau < 10^{-1}$ for typical stars evolving from (late-type) main-sequence to red giant phase. An important model parameter is the distance $R_{\rm h}$ in the stellar envelope at which dust grains may form. It depends on radius and effective temperature of the source star as shown in Section 4.1.

With this in hand, we can evaluate the polarization profile $P(t)$ during a microlensing event. It turns out that the ratio $\bar{R}_{\rm h}/u_0$ determines both the strength (apart the dependence of P on τ) and the shape of the expected polarization signal.

In particular, when $\bar{R}_{\rm h}/u_0 < 0.75$, i.e. for *bypass* events, the polarization $P(t)$ shows a bell-like profile with the peak occurring at t_0. As shown in Fig. 1, the actual value of $P_{\max}(t_0)/\tau$ depends on the ratio $\bar{R}_{\rm h}/u_0$, being $P_{\max}(t_0)/\tau \simeq 12.5$ per cent at $\bar{R}_{\rm h}/u_0 \simeq 0.75$.

For $\bar{R}_{\rm h}/u_0 > 0.75$, i.e. for *transit* events, the polarization curve presents a central minimum (in correspondence to t_0), while two maxima occur at the time instants $t_{\rm h} = t_0 \pm t_{\rm E}\sqrt{(\bar{R}_{\rm h}/0.75)^2 - u_0^2}$ at which the internal cavity (of the stellar atmosphere devoid of dust, projected in the lens plane) enters and exits the lens. The maximum polarization degree is again $P_{\max}(t_{\rm h})/\tau \simeq 12.5$ per cent, corresponding to a lens–source projected distance $u_{\rm h} = 0.75u_0$.

Clearly, with this in mind, one can predict in advance for which events and at which time the observing resources may be focused to make a polarization measurement in an ongoing microlensing event.

The Monte Carlo analysis shows how $P_{\max}$ depends on the stellar parameters (see Figs 4, 5 and 6): $P_{\max}$ increases from (late-type) main-sequence to AGB star phase increasing from 10^{-3} up to values of a few per cent. Our analysis also shows that the *transit* events have a higher polarization degree with respect to *bypass* ones and that the same level of $P_{\max}(t_{\rm h})$ is achieved irrespectively on the u_0 value.

However, the combined analysis with the OGLE-III events clearly shows the absence of events with expected polarization $P_{\rm max} > 1$ per cent, as a consequence of the paucity of AGB stars in the Galactic bulge. Therefore, an observational programme devoted to measure the polarization in an ongoing microlensing event must be designed to be able to measure a polarization degree $P_{\rm max} \gtrsim 0.1$ per cent, that is the threshold value (in 1 h integration time) for the FORS2 polarimeter at VLT telescope. Stated this, we find that, as shown in Fig. 8, about two dozen of events (about 1 per cent of the OGLE-III events) have $P_{\rm max} > 0.1$ per cent and apparent magnitude $I < 14.5$ at the instant $t_{\rm h}$ of the polarization peak. This makes realistic the possibility to measure the polarization in about a few events per year with the present observational capabilities (OGLE-III like). Of course, increasing the event rate (up to thousands per year) as expected in the forthcoming programs *EUCLID*, *WFIRST* and KMTNet, the chance to pick-up events with large ($P > 0.1$ per cent) polarization correspondingly increases.

After the initial submission of the present manuscript Sajadian & Rahvar (2014) presented an analysis of the expected polarization signal in the OGLE-III data set. Although discussed within a different framework of our analysis, their main conclusions are in agreement with those discussed in this work. Specifically, a few per cent of microlensing events towards the Galactic bulge may indeed show up detectable polarization signals.

ACKNOWLEDGEMENTS

We acknowledge for stimulating discussions N. Rattenbury and H. M. Schmid. We also thank the anonymous referee for useful comments. This work make use of the IAC-Star synthetic CMD computational code. IAC-Star is supported and maintained by the computer division of the Instituto de Astrofisica de Canarias.

REFERENCES

Abe F. et al., 2003, A&A, 411, L493
Agol E., 1996, MNRAS, 279, 571
Alcock C. et al., 1997, ApJ, 491, 436
Bogdanov M. B., Cherepashchuk A. M., Sazhin M. V., 1996, Ap&SS, 235, 219
Calchi Novati S., 2010, Gen. Relativ. Gravit., 42, 2101
Calchi Novati S. et al., 2014, ApJ, 783, 86, 2014
Catelan M., 2000, ApJ, 531, 826
Chandrasekhar S., 1950, Radiative Transfer. Clarendon Press, Oxford
Choi J.-Y. et al., 2012, ApJ, 751, 41
Dominik M., 2010, Gen. Relativ. Gravit., 42, 2075
Draine B. T., Lee H. M, 1984, ApJ, 285, 89
Einstein A., 1936, Science, 84, 506
Ferguson J. W., Alexander D. R., Allard F., Barman T., Bodnarik J. G., Hauschildt P. H., Heffner-Wong A., Tamanai A., 2005, ApJ, 623, 585
Flury D. M., Stenflo J. O., 1999, A&A, 341, 902
Gaudi B. S., 2010, in Seager S., ed., Exoplanets. Univ. Arizona Press, Tucson, AZ, p. 79
Gaudi B. S., Gould A., 1999, ApJ, 513, 619
Henderson C. B. et al., 2014, ApJ, 794, 71
Heyrovský D., Sasselov R. D., 2000, ApJ, 529, 69
Ignace R., Bjorkman E., Bryce H. M., 2006, MNRAS, 366, 92
Ignace R., Bjorkman E., Bunker C., 2008, in Kerins E., Mao S., Rattenbury N., Wyrzykowski L., eds, Proceedings of the Manchester Microlensing Conference: The 12th International Conference and ANGLES Microlensing Workshop, PoS(GMC8)002 (http://pos.sissa.it/archive/conferences/054/027/GMC8_027.pdf)
Ingrosso G., Calchi Novati S., De Paolis F., Jetzer Ph ., Nucita A. A., Strafella F., 2006, A&A, 445, 375
Ingrosso G., Calchi Novati S., De Paolis F., Jetzer Ph., Nucita A. A., Scarpetta G., Strafella F., 2007, A&A, 462, 895
Ingrosso G., Calchi Novati S., De Paolis F., Jetzer Ph., Nucita A. A., Zakharov A. F., 2009, MNRAS, 399, 219
Ingrosso G., Calchi Novati S., De Paolis F., Jetzer Ph., Nucita A. A., Strafella F., Zakharov A. F., 2012, MNRAS, 426, 1496
Ingrosso G. et al., 2014, Phys. Scr., 89, 4001
Kroupa P., Tout C. A., Gilmore G., 1993, MNRAS, 262, 545
Lamers H. J., Cassinelli J. P., 1999, Introduction to Stellar Winds. Cambridge Univ. Press, Cambridge
Marshall J. R., van Loon J. Th., Matsuura M., Wood P R., Zijlstra A. A., Whitelock P. A., 2004, MNRAS, 355, 1348
Mathis J. S., Rumpl W., Nordsiek K. H., 1977, ApJ, 217, 425
Moniez M., 2010, Gen. Relativ. Gravit., 42, 2047
Nataf D. M. et al., 2013, ApJ, 769, 88
Paczyński B., 1986, ApJ, 304, 1
Penny M. T. et al., 2013, MNRAS, 434, 2
Reimers D., 1975, Mem. Soc. R. Sci. Liegi, 8, 369
Sajadian S., Rahvar S., 2014, MNRAS, preprint (astro-ph/1409.2653v1)
Schneider P., Wagoner R. V., 1997, ApJ, 314, 154
Schneider P., Weiss A., 1992, A&A, 260, 1
Schneider P., Ehlers J., Falco E. E., 1992, Gravitational Lensing. Springer-Verlag, Berlin
Sekiguchi M., Fukugita M., 2000, ApJ, 120, 1072
Simmons J. F. L., Newsam A. M., Willis J. P., 1995a, MNRAS, 276, 182
Simmons J. F. L., Willis J. P., Newsam A. M., 1995b, A&A, 293, L46
Simmons J. F. L., Bjorkman J. E., Ignace R., Coleman I. J., 2002, MNRAS, 336, 501
Wyrzykowski L. et al., 2014, ApJS, preprint (arXiv:1405.3134)
Yee J. C. et al., 2014, preprint (arXiv:1409.2759)
Yoshida H., 2006, MNRAS, 369, 997
Zakharov A. F., 1995, A&A, 293, 1

This paper has been typeset from a TEX/LATEX file prepared by the author.